Few Layer Reduced Graphene Oxide: Evaluation of the Best Experimental Conditions for Easy Production

Giovani Pavoski[a], Thuany Maraschin[b], Fabiana de Carvalho Fim[a,c], Naira Maria Balzaretti[d],

Griselda Barrera Galland[a], Cássio Stein Moura[e], Nara Regina de Souza Basso[b]*

[a] *Instituto de Química, Universidade Federal do Rio Grande do Sul – UFRGS, Av. Bento Gonçalves, 9500, 91570-970, Porto Alegre, RS, Brazil*
[b] *Faculdade de Química, Pontifícia Universidade Católica do Rio Grande do Sul – PUCRS, Av. Ipiranga, 6681, 90619-900, Porto Alegre, RS, Brazil*
[c] *Centro de Tecnologia, Universidade Federal da Paraíba – UFPB, Cidade Universitária, s/n, 58051-900, João Pessoa, PB, Brazil*
[d] *Instituto de Física, Universidade Federal do Rio Grande do Sul – UFRGS, Av. Bento Gonçalves, 9500, 91570-970, Porto Alegre, RS, Brazil*
[e] *Faculdade de Física, Pontifícia Universidade Católica do Rio Grande do Sul – PUCRS, Av. Ipiranga, 6681, 90619-900, Porto Alegre, RS, Brazil*

This work aimed to produce graphene oxide with few graphene layers, a low number of defects, good conductivity and reasonable amount of oxygen, adequate for use as filler in polymeric composites. Two starting materials were evaluated: expanded graphite and graphite flakes. The method of oxidation used was the Staudenmaier one, which was tested over different lengths of time. No appreciable differences were found among the oxidation times and so the lowest oxidation time (24 h) was chosen as the most adequate. An investigation was also conducted into suitable temperatures for the reduction of graphite oxide. A temperature of 1000 ºC gave the best results, allowing a good quality material with few defects to be obtained. The reduction was also evaluated under inert and normal atmosphere. The best results were obtained when the least modified material, e. g., graphite flakes, was used as a starting material, oxidized for 24h and reduced at 1000 ºC for 30 s in a quartz ampoule under a normal atmosphere.

1. Introduction

Research on new materials has grown exponentially in recent decades due to the requirements of manufacturers in industry and a plethora of new uses, even in social life. Graphene—a single sheet of carbon atoms organized in a planar bi-dimensional network—is part of a special class of nanofillers with the potential to be used in composites. Graphene, or few layer graphene, can be obtained from graphite (stacked layers of graphene), a low-cost starting material that is found in nature as flakes or a powder with diverse particle sizes. The three largest producers of graphite are China, India and Brazil[1]. Andre Geim and Konstantin Novoselov made an outstanding contribution to the study of graphene's properties and received the Nobel Prize of Physics in 2010 for their innovative experiments[2,3]. They discovered that graphene is 200 times stronger than steel and conducts electricity at room temperature faster than any other known material. It is also highly transparent (97.3%) and extremely lightweight. Due to these remarkable properties, a large variety of applications seems possible, including the creation of new materials and innovative electronic products[4]. The properties of graphene are very dependent on its structure and therefore it is of great importance investigating methodologies for producing large quantities of single layer graphene. A structured material with a little number of layers of graphene is acceptable as well. In any case, for nanotechnology applications a little amount of defects is mandatory.

The routes to producing graphene include *bottom-up* and *top-down* processes. The *bottom-up* process is related to the synthesis of the material, while the *top-down* process refers to graphite exfoliation and it is performed until the desired number of graphene layers is achieved[5]. Chemical and mechanical exfoliation of graphite are the only possible methods for obtaining graphene in large quantities and at a low cost[6]. Chemical exfoliation promotes the oxidation of graphite through the introduction of functional groups such as hydroxyl, carbonyl, and epoxide. These groups decrease the interactions between the graphene layers, resulting in an increase of the interlayer distance. The larger space between the graphene sheets helps in carrying out exfoliation, leading to the formation of monolayer or few layers graphene oxide (GO). Electrical properties are influenced by the degree of oxidation and by the surface chemistry of the GO powders[7].

* e-mail: nrbass@pucrs.br

Some authors compared the most commonly used oxidation processes, e. g., the Staudenmaier[10], Hofmann[11] and Hummers[12] methods, and showed that the Staudenmaier method produces thermally reduced graphene with the lowest proportion of defects. A comparison of the electrochemical performance of the graphene samples obtained from each of these three oxidation methods and a reduction at 1000ºC showed that the sample prepared using the Hummers method presented higher heterogeneous transfer rates and lower overpotentials compared with the samples obtained via the other two methods. These data indicate that the preparation method has a dramatic influence on the properties of graphene[13]. Some studies have modified the Staudenmaier process by experimenting with the oxidation time (between 1 and 7 days) and the $HNO_3:H_2SO_4$ acids ratio (1:2 and 1:3), with the aim of obtaining graphene oxide with optimum interlayer spacing. It was found that the optimal conditions were obtained with $HNO_3:H_2SO_4$ at a 1:3 volume ratio after 96 h of oxidation. The interlayer distances could be increased from 3.55 Å of the original graphite to 9.13 Å in modified Staudenmaier method[12]. However, the required reaction time to achieve the appropriate level of intercalation and oxidation also depends on the starting flake size[15]. Aksay et al[16]. found that 96 h of oxidation reaction was enough to completely oxidize 45 μm flakes but insufficient for 400 μm flakes. Oxygen can be eliminated partially through the thermal or chemical reduction of GO[17], resulting in reduced graphene oxide. However, it must be considered that the reduced GO may present defects in the crystalline network that can affect the graphene's electrical properties negatively[18]. Accordingly, intensive research into improving the methodologies for reducing GO and restoring the conductive network is being undertaken[19]. Existing studies have looked at thermal reduction at high temperatures (1050 °C)[16,20] and at low temperatures (125-240 °C) [21,22], whilst other works have examined the influence of the amount of carbon and oxygen on conductivity after thermal reductions at 900°C and 1100°C [23]. Many of these studies are difficult to compare because they use different oxidation methods and reduction conditions. Diffusion coefficient calculations suggest that there is a critical temperature of 550 ºC that must be exceeded for exfoliation to occur [23]. The present work aims to develop a methodology for obtaining large quantities of few layer reduced graphene oxide from graphite at a low cost, while presenting good quality and a reasonable amount of oxygen, which could be used as nanofiller for composites[24]. Since the starting material plays an important role, we decided to compare two materials: graphite flakes (FK) and expanded graphite (EG). The oxidation process used was the Staudenmaier[10] method. Various reaction times were tested (24, 48, 72 e 96h). Thermal reduction processes at 600, 700, and 1000 °C, in different atmospheres (normal and inert), were also investigated.

2. Experimental

2.1. Materials

All materials were used as received. Expanded graphite Micrograph HC11 (EG) with an average size of around 50 μm and Graflake 9950 (FK) with a size of around 150 μm were provided by Nacional de Grafite Ltda. Brazil. Sulfuric acid, nitric acid, hydrochloric acid, and potassium chlorate were purchased from Merck Chemical Company (Brazil).

2.2. Graphite Oxide Synthesis

The graphite oxide (GO) was synthesized from EG and FK powders using the Staudenmaier method[10]. An acidic mixture of H_2SO_4 (160 mL) and HNO_3 (90 mL) was stirred in a round-bottomed flask placed in an ice bath for 1 h. After this time, 10g of graphite (EG or FK) were added and stirred for 20 min. Subsequently, 110g of $KClO_3$ was added slowly over 15 mins, with the temperature being controlled to prevent a rise above 35°C. Small amounts of KCl were added to minimize the risk of explosion, which can be caused by the ClO_2 gas. The reaction was allowed to proceed over different intervals of time (24, 48, 72 e 96h). On completion of the reaction, an aqueous HCl solution (10% v/v) was added to the suspension in order to remove sulfate ions. Afterwards, washing with deionized water and centrifuging (4500 rpm) were carried out several times in order to reach pH 3. The resulting suspension was placed in a dialysis membrane until the pH of solution was 5, and then the resulting brown suspension was dried in an oven at 150°C. The graphite oxide was then heated at 600, 700, and 1000ºC for 30 s in an oven, using a closed quartz ampoule with either a normal or an inert atmosphere of argon.

2.3. Characterization

X-ray diffraction (XRD) measurements for the powdered samples were performed on a diffractometer (Rigaku, DMAX 2200) equipped with a Cu tube (λ = 0.15418 nm) and a secondary monochromator. The goniometer used was a Siemens D500 and the detector was the scintillator (NaI and Tl). XRD samples were prepared by coating the sample holder with a uniform layer of the powdered samples at room temperature. From the XRD parameters, the interlayer distances (d_{002}) in the graphene were estimated using Bragg's Law [25].

The grain size (C) was calculated using the Scherrer equation[26, 27]:

$$C = \frac{0.9\lambda}{\beta \cos\theta}$$

Here, β is the line width at half height in the radians and θ is the diffraction angle.

The number of graphene layers was calculated by dividing the crystal size (C) by the interlayer distance (*d*) added to the thickness of one graphene sheet (0.1 nm).

Raman analyses were performed at room temperature using an Olympus microscope and an iH320 Jobin Yvon Spectrometer with a CCD (charged coupled device) detector, cooled by liquid nitrogen. The excitation source was a 10 mW HeNe laser (632.8 nm) and the acquisition time was 20 s.

GO samples were analyzed at 25 °C as pellets diluted in KBr by transmission FT-IR spectroscopy, using a Varian FTIR spectrophotometer (640-IR), which accumulated 32 scans at a 4 cm^{-1} resolution.

The fractions of C, H, and N in the graphite samples were analyzed using a Perkin-Elmer MCHNSO/2400 analyzer. A sample mass of 2 mg was employed in each analysis.

Scanning Electron Microscopy (SEM) was performed with a Phillips microscope (model XL30) operating at 20 kV, using aluminum stubs and gold metallization.

Transmission Electron Microscopy (TEM) images of the reduced graphene oxide were obtained using a JEOL 2010 transmission electron microscope operated at 200 kV. All the samples were prepared by depositing an acetone suspension drop on a copper grid (300 mesh) covered with amorphous carbon.

Electrical impedance spectroscopy was performed to measure the electrical conductivity of the samples. A sine wave with 1.0 Vpp was applied to the sample and the frequency was varied from 1 to 10^6 Hz. The current and the potential differences between the samples' faces were measured. The phase difference between the voltage and current in the sample allows the determination of the real and imaginary parts of electrical impedance. The real part is associated with conductivity. A numerical fitting algorithm was applied to the data, which provided the conductivity values.

3. Results and Discussion

In order to evaluate the need for pre-treatment in the oxidation process, two different types of graphite were employed as starting materials: expanded graphite (EG) and graphite flake (FK). Figure 1 shows the XRD patterns of EG and FK. It is possible to observe the interlayer spacing along the c-axis—(d$_{002}$) at 26.5º and (d$_{004}$) at ~55º—as sharp peaks for FK. In Table 1, it can be seen that both graphites present a very close spacing between the graphene layers but the crystal size of EG is smaller, which indicates a smaller graphene stack. The inexistence of peak at 55º in EG suggests it has a lower aspect ratio than FK.

Raman spectroscopy is commonly considered to be the most important technique in characterizing the structure of graphitic materials[28]. The main Raman features of graphene and graphite are the G band (~1580 cm^{-1}), the D band (~1330 cm^{-1}) and the G´ band (~2670 cm^{-1}) for an excitation wavelength of 632.8 nm. The G band originates from the

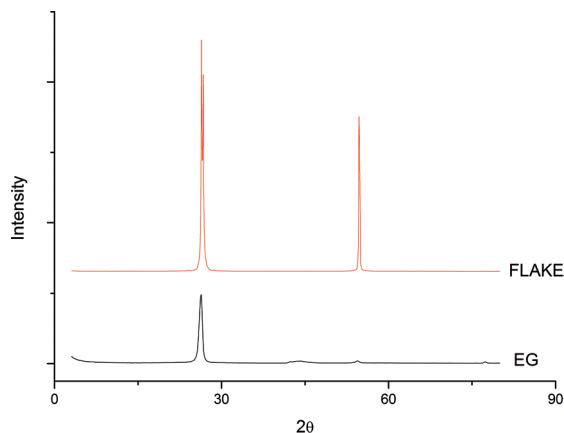**Figure 1:** XRD patterns of starting graphite materials

Table 1: Data obtained from the XRD patterns of EG and FK

Sample	2θ (º)	d$_{002}$ (nm)	C (nm)
EG	26.52	0.3390	14
Flake	26.55	0.3356	17

in-plane vibration of sp^2 carbon atoms. The D band is related to crystal disorder due to sp^3 defects in the sp^2 lattice and the G´ band is an overtone of the disorder-induced D-band. For single layer graphene, the G´ band appears as a sharp and symmetrical peak, whereas it becomes broader when the thickness increases (for example, in few layer graphene)[29]. Figure 2 shows the Raman spectra of the two types of graphitic structures used in this work, namely, FK and EG. It can be observed that both structures present defects (peak D at 1330 cm^{-1}). The larger and less intense G´ band suggests that the EG sheets contain more defects compared to the FK sheets.
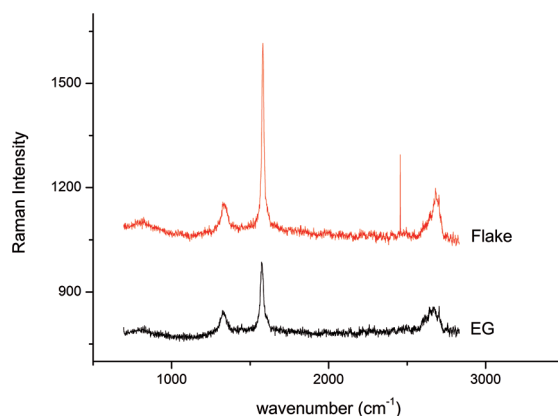

Figure 2: Raman spectra of starting graphite materials

3.1. Reduced graphene oxide obtained from expanded graphite

The strong oxidation of EG using Staudenmaier methodology over 96 h resulted in graphite oxide (GO96h). The formation of GO is indicated by the increase of the interlayer spacing along the c-axis (d$_{002}$) due to the insertion of

various oxygen-containing functional groups in the graphite structure[2]. Figure 3 shows the XRD patterns of GO prepared from EG oxidation.

The data listed in Table 2 refers to the parameters of XRD and the percentage of carbon and oxygen obtained from CHN analysis for EG, GO96h and reduced GO at different temperatures (600, 700 or 1000°C).

The formation of GO96h is confirmed by the absence of the (002) diffraction line at 26.52º (d-space = 0.33 nm) that is typical of EG and the appearance of the diffraction peak at 11.23° (d-space = 0.78 nm) (Figure 3). Moreover, a marked decrease in the crystal size (8 nm) compared to the starting graphite (14 nm) was also observed. During the oxidation process, the insertion of various oxygen-containing functional groups that are bonded to the edges of basal planes of the graphite structure occurs. The ratio between the carbon and oxygen obtained by CHN analysis shows that oxidation was almost complete after 96 h (C/O ≅ 1). A high percentage of oxygen is very important for the expansion and exfoliation of graphene sheets, since the percentage represents the number of molecules that will decompose in gases during thermal treatment[15]. Aksay et al.[16] determined the composition of gases that cause the rapid expansion of graphite—namely, CO_2 and H_2O—demonstrating they originate from the exothermic decomposition of the hydroxyl and epoxide groups of GO.

When EG is oxidized to become GO, the insertion of oxygen functional groups decreases electrical conductivity due to a disruption in the planar sp^2 carbon sheets because of the introduction of sp^3-hybridized carbons[5]. In order to restore the π-network, the GO was submitted to thermal reduction and the influence of the reduction temperature on the reduced graphene oxide was evaluated. The thermal treatments were carried out in an oven using a quartz ampoule.

Figure 4 shows the XRD patterns of GO96h samples that were heated at 600, 700, and 1000 °C (GO96h6, GO96h7, and GO96h10, respectively). All the reduced GO samples showed a broad peak that corresponded to 0.78 nm GO interlayer separation, indicating that the reduction process was not complete. A very large peak at 2θ ≅ 26.5° reappeared for the samples reduced at 600 and 700°C, showing that the graphitic structure was partially restored. However, the peak broadens even more for higher temperatures, presumably due to the corrugated structure of the reduced GO sheets. Although the absence of the (002) diffraction line at 2θ = 26.5° in the XRD spectrum of GO96h10 suggests that all stacking was lost, it may also indicate that any remaining stacking was disordered[16].
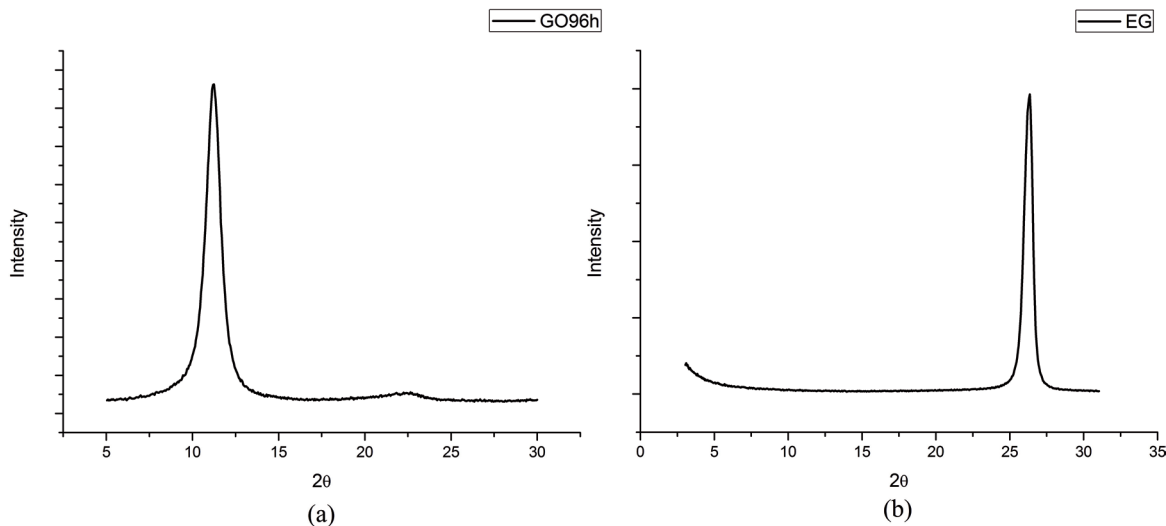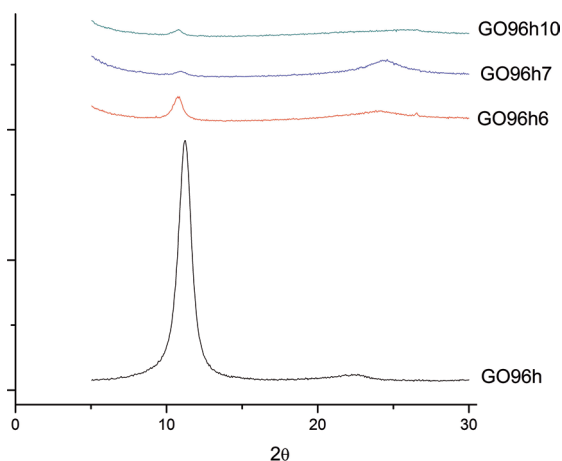

Figure 3: XRD patterns of GO96h (a) and EG (b)

Table 2: Data obtained from the XRD patterns and CHN of EG, GO96h and reduced GO96h at different temperatures.

Sample	2θ (°)		d$_{002}$ (nm)		Grain size C (nm)		CHN	
							%C	%O
EG		26.52		0.33		14	97.5	2.4
GO96h	11.23		0.78		8		49.9	47.8
*GO96h6	10.74	24.14	0.82	0.37	9	3	73.3	25.7
GO96h7	10.95	24.36	0.81	0.37	8	3	74.1	24.7
GO96h10	10.79		0.82		11		80.2	19.0

*GO96h6: correspond to GO 96h that was reduced at 600°C. The same nomenclature was used for the other temperatures.

**Figure 4:** XRD patterns of GO and reduced GO96h at different temperatures

According to Table 2, the data from the elemental analysis is consistent with the results obtained from XRD. An increase in the C/O ratios in the reduced samples can be seen when compared with the starting GO96h (1.0), evidencing a successful thermal reduction. Although oxygen functional groups were still retained in the structure at all the evaluated temperatures, it was observed that the C/O ratio increased with increasing of the reduction temperature.

The oxygen-functionalized graphene sheets present opportunities for several applications, such as the preparation of composites in which those groups can have an important role in the interaction between graphene sheets and the polymeric matrix[7]. Covalent functionalization of graphene with the polymer can improve the dispersion in nanocomposites[8]. For example, some hydroxyl functional groups on the surface of graphene were used to support the catalyst system, in the *in situ* polymerization of ethylene, improving the graphite exfoliation in the polymeric matrix and consequently the nanocomposite properties[9]. Table 2 also shows that the differences in the amount of oxygen in the samples reduced at temperatures of 600 and 700°C are not significant. Even at the highest reduction temperature, 1000ºC, roughly 19% of oxygen atoms remained.

Figure 5 shows the Raman spectra for thermally reduced GO96h. According to the Raman spectra, part of the sp[2] carbon network was restored, though with many defects.

Considering that 96 h of oxidation reaction seems to damage the graphitic structure of EG excessively, shorter reaction times (24, 48, and 72 h) were evaluated with the purpose of reducing the defects in the graphene sheets obtained after thermal reduction. However, after thermal reduction of the GO samples at 1000°C, the Raman spectra showed no significant differences, when compared with using an oxidation time of 96 h (see Figure 6).

In fact, these Raman spectra show that a shorter EG oxidation time neither reduces the prevalence of defects, nor affects the stacking ordering. The sp[2] structure, therefore, is not recovered completely during the reduction process.
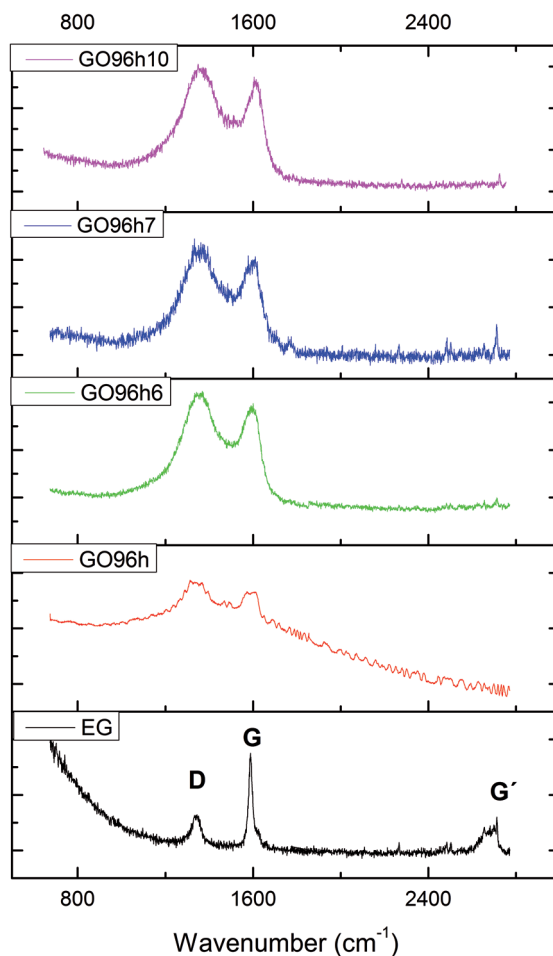
**Figure 5:** Raman spectra of EG, GO96h and reduced GO at 600, 700 and 1000 °C
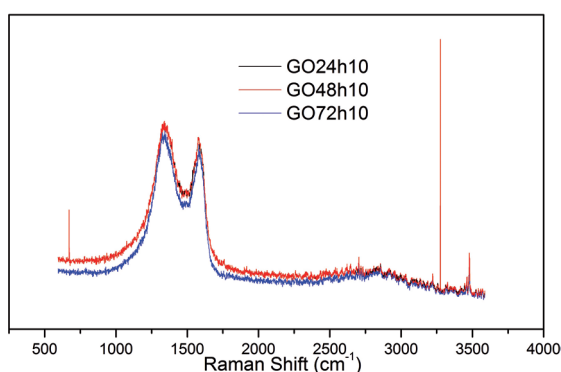
Figure 6: Raman spectra of EG oxidized over different reaction times (24, 48, and 72h) and reduced at 1000 °C

Considering the EG exfoliation, it is possible to conclude that a high degree of oxidation was obtained even after the lowest period of oxidation (24 h), giving C/O ratios close to 1, reducing the crystal size, and increasing interlayer distances. However, even at the highest temperature (1000ºC), the reduction was insufficient for recuperating the sp[2] network, thus leading to the production of few layer reduced graphene oxide with many defects.

3.2. Reduced graphene oxide from graphite flake

Using the same experimental approach as for EG, GO samples were prepared from graphite flakes (FK). Different oxidation times (96, 72, 48, and 24 h) were evaluated. Figure 7 shows some of the typical XRD patterns for GO obtained from FK.
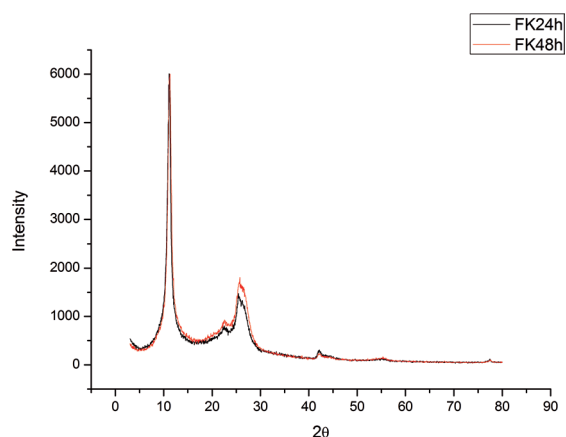
**Figure 7:** XRD patterns of FK oxidized over 24 (FK24h) and 48 h (FK48h)

In contrast to what was observed with EG, FK was only partially oxidized over all the evaluated reaction times. The existence of fewer defects in the FK structure relative to EG may affect the oxidative breakup and a time longer than 96 hours may be required for complete oxidation to occur [16]. Elemental analysis was performed on the graphene oxides in order to evaluate the degree of oxidation (Table 3).

Table 3: Elemental analysis of GO obtained from different lengths of oxidation time.

Sample	%C	%H	%N	%O
FK24h	64.6	2.0	0.7	32.6
FK48h	62.3	2.1	0.7	34.8
FK72h	68.8	1.6	0.6	28.9
FK96h	68.0	1.6	0.7	29.6

According to Table 3, the degree of oxidation was practically independent of the reaction time. It is possible to conclude, therefore, that a 24-hour period of oxidation is long enough to prepare oxidized graphite flake with about 30% oxygen.

The FTIR spectrum of graphite oxide FK24h (presented in Figure 8) shows the stretching vibrations of O-H and C-O at 3398 and 1083cm^{-1} respectively. The stretching C=C double bonds of the condensed rings of graphene appear at 1621cm^{-1}. This band has a shoulder at around 1700cm^{-1} that can be attributed to the presence of some carbonyl groups (C=O) in small amounts. The presence of some stretching vibrations from C-H bonds (C sp^3) is also evident between 2800 and 3000cm^{-1}.
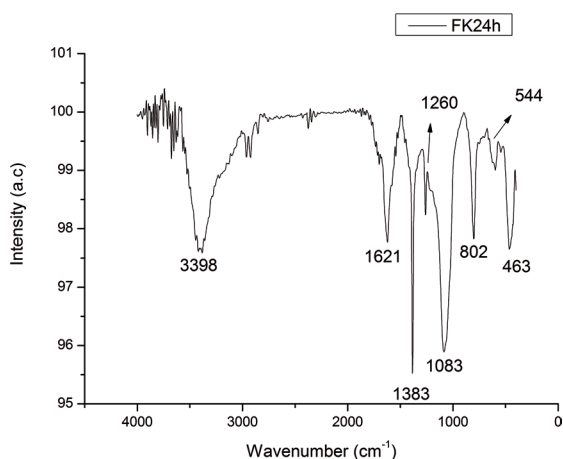

Figure 8: Transmission FTIR spectrum for FK oxidized over 24 h (FK24h), dispersed in KBr

The thermal reduction of the flake oxidized over 24 h was tested at 600, 700, and 1000 ºC. A very simple method of reduction was evaluated using an open quartz capsule placed in the oven. However, this procedure resulted on the loss of the most exfoliated fractions, especially at the highest reduction temperatures. Thus, for the reduction reactions, a closed quartz ampoule was chosen instead, which was tested using normal and inert atmospheres. Figure 9 shows the XRD patterns for the samples obtained after FK was oxidized over 24 h and reduced at 600, 700, and 1000 °C in a closed quartz ampoule, both in an inert atmosphere (FK24h6APIN, FK24h7APIN, FK24h10APIN) and a normal atmosphere (FK24h6AP, FK24h7AP, FK24h10AP). Table 4 gives the XRD patterns for the data obtained.

According to Figure 9, the reduction of GO in an inert atmosphere at temperatures of 600 and 700 °C presents large diffraction peaks, suggesting heterogeneity in the stacking distances. At a reaction temperature of 1000°C, the peak is thinner, even though the average interlayer distance is the same, namely 0.35 nm, which is higher than in the starting graphite (0.33 nm in FK). In all cases, there was significant exfoliation from about 40 graphenes per crystal in FK to 5-11 graphenes per crystal in the reduced graphene oxides. The reduction performed in a closed quartz ampoule in a normal atmosphere was more efficient at a temperature of 1000°C because at 600 and 700°C, there is still a broad diffraction band at 11.29°, which is characteristic of GO. It can thus be seen that the reduction is less efficient at lower temperatures. At a reduction temperature of 1000ºC, the exfoliation is the same in an inert or a normal atmosphere (11 graphenes per crystal).

The Raman spectra in Figure 10 show that the oxidized graphite (FK24h) reduced at 1000°C in a normal atmosphere gives the best recuperation of the sp^2 network, compared with the sample reduced at lower temperatures or in an inert atmosphere. The ratio between the intensities of the D and G peaks is normally used as a quantitative parameter of defect
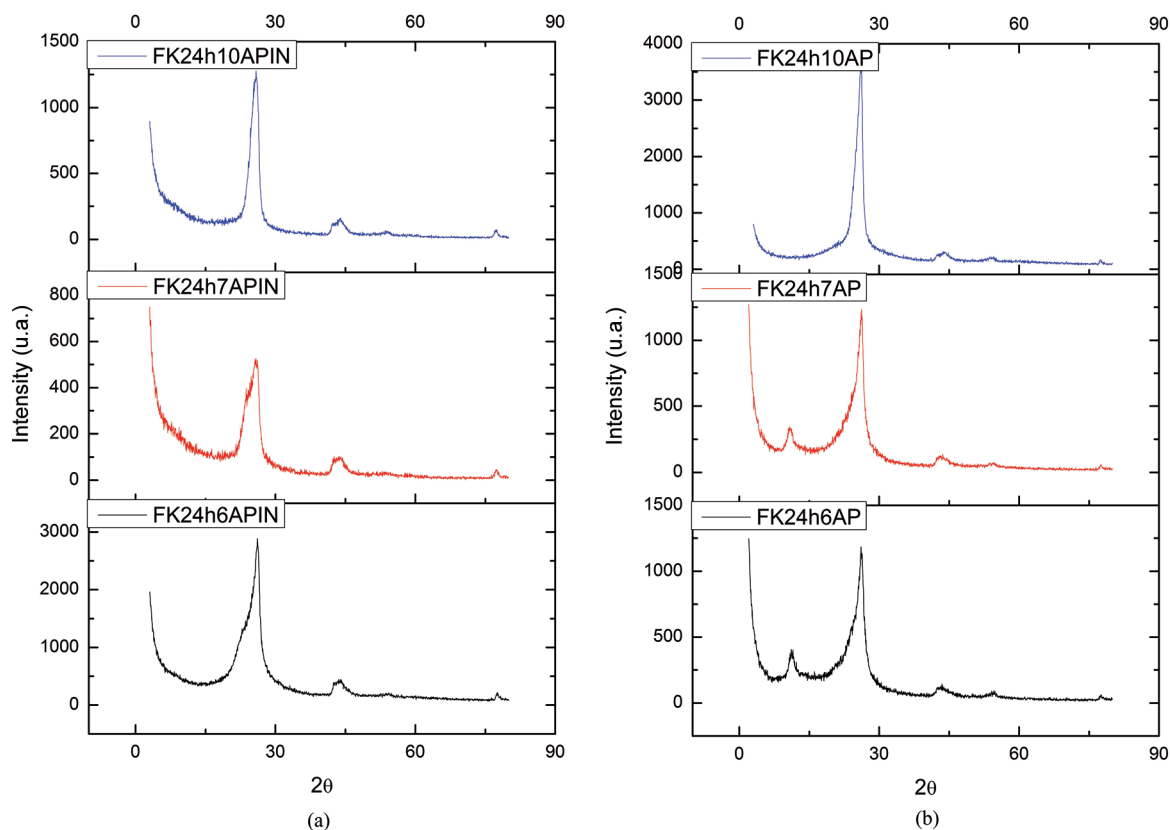
Figure 9: XRD patterns for GO samples reduced in a closed quartz ampoule in (a) an inert (APIN) and (b) a normal (AP) atmosphere

Table 4: Data obtained from the XRD patterns for reduced GO samples treated in a closed quartz ampoule.

Sample	2θ (°)	d (nm)	C (nm)	Graphene #
FK	26.55	0.33	17	40
FK24h6APIN	25.25	0.35	2	5
FK24h6AP	25.65	0.35	3	7
FK24h7APIN	25.08	0.35	3	6
SFK24h7AP	25.67	0.35	9	20
FK24h10APIN	25.52	0.35	5	11
FK24h10AP	25.71	0.35	5	11

prevalence in graphite. In Figure 10, the I_D/I_G ratios for normal and inert atmospheres are 0.8 and 1.1 respectively, confirming the presence of fewer defects in the reduced oxide obtained at 1000ºC in a normal atmosphere, compared with other samples.

According to the results of the elemental analysis (Table 5), an increase in the reaction temperature from 600 to 1000°C raises the C/O ratio, as expected. The use of an inert or a normal atmosphere does not have a significant influence on the amount of oxygen that occurs in the reduced graphite. After reduction at the highest temperature (1000°C), there is still a reasonable amount of oxygen present (13%), which can be used in compatibility reactions for the preparation of composites. In any case, the amount of oxygen is inferior to that obtained when EG is used as a starting material.
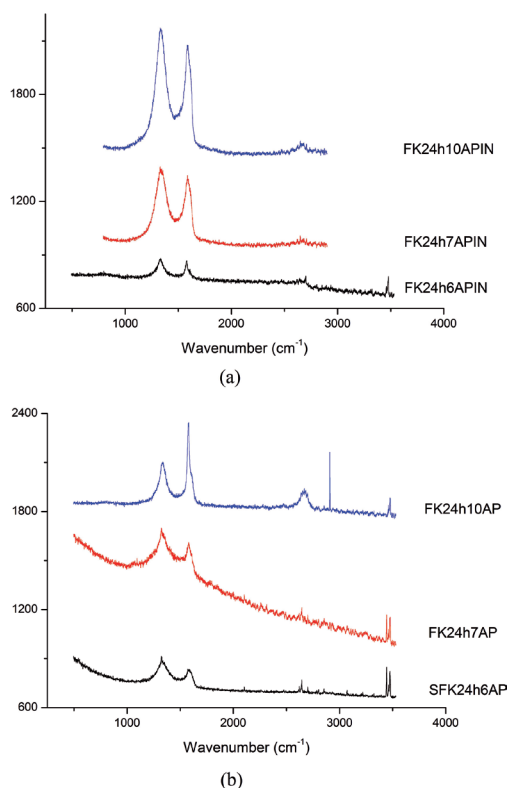
Figure 10: Raman spectra of GO samples reduced in a quartz ampoule in (a) an inert and (b) a normal atmosphere

Table 5: Elemental analysis of reduced GO obtained in a closed ampoule.

Sample	%C	%O
GO	64.7	33.9
FK24h6APIN	72.3	27.0
FK24h7APIN	85.5	14.2
FK24h10APIN	86.7	13.1
FK24h10AP	86.3	13.2

The HRTEM image of the FK24h10AP sample shows a few layer graphene sheet, which indicates that an effective exfoliation of graphite oxide has taken place (Figure 11).
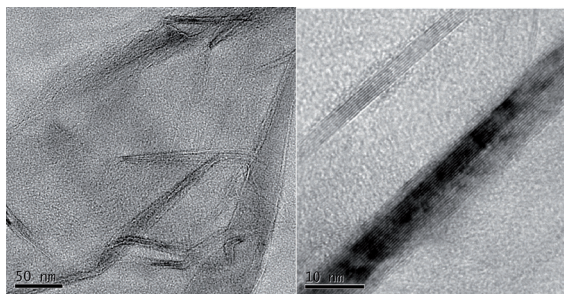

Figure 11: HRTEM micrographic image of oxide graphene oxidized over 24h and thermally reduced at 1000°C in a closed quartz ampoule in a normal atmosphere.

Table 6 shows the conductivity values for the samples, measured by electrical impedance spectroscopy prior to and after reduction treatment. One can observe that the oxidation of the FK decreased the electric conductivity of sample FK24h slightly; however, the reduction process, independent of the temperature, was very efficient in restoring the sp^2 network, which is responsible for conductivity. The oxidation process and the reduction resulted in a material composed of few layer graphene, which is roughly one order of magnitude more conductive than the raw material.

Table 6: Electrical conductivity of raw materials oxidized and reduced graphite.

Sample	Electrical conductivity (S/cm)
FK	6.0×10^{-2}
EG	3.5×10^{-2}
FK24h	1.2×10^{-2}
FK24h6APIN	1.6×10^{-1}
FK 24h7APIN	2.7×10^{-1}
FK24h10PIN	2.7×10^{-1}
FK24h10AP	1.7×10^{-1}

4. Conclusions

Using expanded graphite (50 μm, crystal size 14 nm) as a starting material to obtain reduced graphite oxide produced few layer graphene with many defects. The raw untreated graphite (flake, 150 μm, crystal size 17 nm) was found to be the starting material most appropriate for producing reduced graphene oxide through the modified Staudenmaier method. Reduced graphene oxide containing roughly 13% oxygen, a low density of defects and a low number of graphene layers was obtained from oxidation of the graphite flake over a 24 h period, followed by thermal reduction at 1000 ºC in a quartz ampoule using a normal atmosphere. The use of an inert atmosphere during the reduction process did not improve the structure or electrical properties of the resulting reduced graphene oxide. The electrical conductivity of the few layer graphene obtained was ten times superior to that of the starting graphite.

The few layer graphene material with a low defect density that was obtained is adequate for many applications, such as use in polymeric composites, for example.

5. Acknowledgments

6. References

1. US Geological Survey. *Mineral Commodity Summaries*. Washington: US Department of the Interior; 2013. Available from: <http://minerals.usgs.gov/minerals/pubs/mcs/2013/mcs2013.pdf>. Access in: 15/10/2014.

2. Novoselov KS, Geim AK, Morozov SV, Jiang D, Zhang Y, Dubonos SV, et al. Electric field effect in atomically thin carbon films. *Science*. 2004;306(5696):666-669.

3. The Official Web Site of the Nobel Prize. *The Nobel Prize in Physics 2010.* Nobelprize.org; 2010. Available from: <http://www.nobelprize.org/nobel_prizes/physics/laureates/2010/>. Access in: 04/01/2012.

4. Salavagione HJ, Martinez G, Ellis G. Recent Advances in the Covalent Modification of Graphene with Polymers. *Macromolecular Rapid Communications*. 2011;32(22):1771-1789.

5. Moura CS, Amaral L. Carbon nanotube ropes proposed as particle pipes. *Carbon*. 2007;45(9):1802-1807.

6. Wu ZS, Ren W, Gao L, Liu B, Jiang C, Cheng HM. Synthesis of high-quality graphene with a pre-determined number of layers. *Carbon*. 2009;47(2):493-499.

7. Guerrero-Contreras J, Caballero-Briones F. Graphene oxide powders with different oxidation degree, prepared by synthesis variations of the Hummers method. *Materials Chemistry and Physics*. 2015;153:209-220.

8. Zhang M, Li Y, Su Z, Wei G. Recent advances in the synthesis and applications of graphene-polymer nanocomposites. *Polymer Chemistry*. 2015;6(34):6107-6124.

9. Pavoski G, Maraschin T, Milani MA, Azambuja DS, Quijada R, Moura CS, et al. Polyethylene/reduced graphite oxide nanocomposites with improved morphology and conductivity. *Polymer*. 2015;81:79-86.

10. Staudenmaier L. Verfahren zur Darstellung der Graphitsäure. *Berichte der deutschen chemischen Gesellschaft*. 1898;31(2):1481-1487.

11. Hofmann U, König EZ. Untersuchungen über Graphitoxyd. *Zeitschrift für Anorganische und Allgemeine Chemie*. 1937;234(4):331-336.

12. Hummers WS Jr., Offeman RE. Preparation of graphitic oxide. *Journal of the American Chemical Society*. 1958;80(6):1339.

13. Poh HL, Šaněk F, Ambrosi A, Zhao G, Sofer Z, Pumera M. Graphenes prepared by Staudenmaier, Hofmann and Hummers methods with consequent thermal exfoliation exhibit very different electrochemical properties. *Nanoscale*. 2012;4(11):3515-3522.

14. Sheshmani S, Fashapoyeh MA. Suitable Chemical Methods for Preparation of Graphene Oxide, Graphene and Surface Functionalized Graphene Nanosheets. *Acta Chimica Slovenica*. 2013;60(4):813-825.

15. Jang BZ, Zhamu A. Processing of nanographene platelets (NGPs) and NGP nanocomposites: a review. *Journal of Materials Science*. 2008;43(15):5092-5101.

16. McAllister MJ, Li JL, Adamson DH, Schniepp HC, Abdala AA, Liu J, et al. Single Sheet Functionalized Graphene by Oxidation and Thermal Expansion of Graphite. *Chemistry of Materials*. 2007;19(18):4396-4404.

17. Schniepp HC, Li J, McAllister MJ, Sai H, Herrera-Alonso M, Adamson DH, et al. A Functionalized Single Graphene Sheets Derived from Splitting Graphite Oxide. *The Journal of Physical Chemistry B*. 2006;110(17):8535-8539.

18. Stankovich S, Dikin DA, Piner RD, Kohlhaas KA, Kleinhammes A, Jia Y, et al. Synthesis of graphene-based nanosheets via chemical reduction of exfoliated graphite oxide. *Carbon*. 2007;45(7):1558-1565.

19. Herrera-Alonso M, Abdala AA, McAllister MJ, Aksay IA, Prud'homme RK. Intercalation and Stitching of Graphite Oxide with Diaminoalkanes. *Langmuir*. 2007;23(21):10644-10649.

20. Becerril HA, Mao J, Liu Z, Stoltenberg RM, Bao Z, Chen Y. Evaluation of Solution Processed Reduced Graphene Oxide Films as Transparent Conductors. *ACS Nano*. 2008;2(3):463-470.

21. Jung I, Dikin DA, Piner RD, Ruoff RS. Tunable Electrical Conductivity of Individual Graphene Oxide Sheets Reduced at "Low" Temperatures. *Nano Letters*. 2008;8(12):4283-4287.

22. Jin M, Jeong HK, Kim TH, So KP, Cui Y, Yu WJ, et al. Synthesis and systematic characterization of functionalized graphene sheets generated by thermal exfoliation at low temperature. *Journal of Physics D: Applied Physics*. 2010;43(27):275402.

23. Pei S, Cheng HM. The reduction of graphene oxide. *Carbon*. 2012;50(9):3210-3228.

24. Mural PKS, Sharma M, Madras G, Bose S. A critical review on *in situ* reduction of graphene oxide during preparation of conducting polymeric nanocomposites. *RSC Advances*. 2015;5(41):32078-32087.

25. Aladekomo JB, Bragg RH. Structural transformations induced in graphite by grinding: Analysis of 002 X-ray diffraction line profiles. *Carbon*. 1990;28(6):897-906.

26. Scherrer P. Bestimmung der Grösse und der inneren Struktur von Kolloidteilchen mittels Röntgenstrahlen. *Nachrichten von der Gesellschaft der Wissenschaften zu Göttingen, Mathematisch-Physikalische Klasse*. 1918;1918(2):98-100.

27. Sahoo SK, Mallik A. Simple, fast and cost-effective electrochemical synthesis of few layer graphene nanosheets. *NANO*. 2014;10(2):1550019.

28. Li ZQ, Lu CJ, Xia ZP, Zhou Y, Luo Z. X-ray diffraction patterns of graphite and turbostratic carbon. *Carbon*. 2007;45(8):1686-1695.

29. Ni Z, Wang Y, Yu T, Shen Z. Raman spectroscopy and imaging of graphene. *Nano Research*. 2008;1(4):273-291.